AD 732463

Technical Report: NAVTRADEVCEN IH-184

FM SONAR SIMULATION TECHNIQUES

Matthew F. Borg
Undersea Warfare Trainers Department
and
Francis Murphree
Electronics Laboratory

Naval Training Device Center
Orlando, Florida 32813

February 1971

DoD Distribution Statement

Approved for public release; distribution is unlimited.

NAVAL TRAINING DEVICE CENTER

ORLANDO, FLORIDA

38

UNCLASSIFIED NAVTRADEVCEN IH-184
Security Classification

DOCUMENT CONTROL DATA - R & D	
1. ORIGINATING ACTIVITY (Corporate author) Naval Training Device Center Orlando, Florida 32813	2a. REPORT SECURITY CLASSIFICATION UNCLASSIFIED; 2b. GROUP
3. REPORT TITLE FM Sonar Simulation Techniques	
4. DESCRIPTIVE NOTES (Type of report and inclusive dates) Final Report April 1970	
5. AUTHOR(S) (First name, middle initial, last name) Matthew P. Borg and Francis Murphree	
6. REPORT DATE April 1970	7a. TOTAL NO. OF PAGES 31; 7b. NO. OF REFS 16
8a. CONTRACT OR GRANT NO. b. PROJECT NO. NAVTRADEVCEN Task No. 8207 c. d.	9a. ORIGINATOR'S REPORT NUMBER(S); 9b. OTHER REPORT NO(S) (Any other numbers that may be assigned this report) NAVTRADEVCEN IH-184
10. DISTRIBUTION STATEMENT Approved for public release; distribution unlimited.	
11. SUPPLEMENTARY NOTES	12. SPONSORING MILITARY ACTIVITY Naval Training Device Center Orlando, Florida 32813

13. ABSTRACT

This report outlines technical areas needed for the development of a Continuous Transmission Frequency Modulated Sonar Operator Trainer.

The report discusses the contents of a possible standardized active sonar equation to be used in the mathematical modeling of the transmitted and received signal. There is also outlined a hybrid computer technique for producing artificial signals to stimulate the display consoles with dynamic sonar echo returns of mine, non-mine and subterranean targets and features.

14. KEY WORDS	LINK A		LINK B		LINK C	
	ROLE	WT	ROLE	WT	ROLE	WT
Simulation						
Sonar, FM, CT						
Target echo simulation						
PPI displays						
Hybrid computer						
Underwater acoustics						

Technical Report: NAVTRADEVCEN IH-184

FM SONAR SIMULATION TECHNIQUES

ABSTRACT

This report outlines technical areas needed for the development of a Continuous Transmission Frequency Modulated Sonar Operator Trainer.

The report in Section 1 discusses the contents of a possible standardized active sonar equation to be used in the mathematical modeling of the transmitted and received signal. There is also outlined in Section 2 a hybrid computer technique for producing artificial signals as inputs to the display consoles with dynamic sonar echo returns of mine, non-mine and subterranean targets and features.

TECHNICAL REPORT: NAVTRADEVCEN 1H-184

FM SONAR SIMULATION TECHNIQUES

MATTHEW F. BORG
UNDERSEA WARFARE TRAINERS DEPARTMENT

and

FRANCIS MURPHREE
ELECTRONICS LABORATORY

APRIL 1970

APPROVED:

HEAD, UNDERSEA WARFARE TRAINERS DEPT

HEAD, ELECTRONICS LABORATORY

MR. J. C. WOOTTON
ASSOCIATE TECHNICAL DIRECTOR

DR. H. H. WOLFF
TECHNICAL DIRECTOR

NAVAL TRAINING DEVICE CENTER
ORLANDO, FLORIDA

TABLE OF CONTENTS

LIST OF ILLUSTRATIONS

SECTION I

SIMULATION, FOR TRAINING PURPOSES, OF THE CONTINUOUS TRANSMISSION FREQUENCY MODULATED (CTFM) SONAR

By MATTHEW F. BORG

1. INTRODUCTION

Comprehensive mine hunting sonar shipboard training in the active mode for classification of mine and non-mine targets with CTFM type sonars is not practicable. The more important reasons for this statement are lack of suitable targets and lack of insitu identifications. These reasons are particularly applicable for submarine sonars when used for mine avoidance or close contract avoidance. In addition, training in which sea floor, subterranean features and polar ice patterns are introduced into the displays, is a distinct necessity for submarine sonarmen. A shorebased device is the only practicable means of providing this training.

Efforts in providing artificial target data to CTFM sonars, either for shorebased or shipboard use are limited to a magnetic tape recorder/reproducer unit recently developed by the Naval Undersea Warfare Center, San Diego, California. This tape recorder will interface with the AN/BQS-8 sonar. Additionally, an obsolete trainer developed in World War II is shown in reference (1). There is no operational CTFM sonar training device in use today at any shorebased training school.

This report will outline certain technical areas needed in anticipation of future contractual work in developing a CTFM sonar trainer. The technique for generating the sonar signals will be by Hybrid Computer. In support of this form of simulation, the report will discuss the contents of a possible standardized active sonar equation; shapes of Plan Position Indicator (PPI) echo returns of mine, non-mine objects and subterranean features, and finally an electronic technique for interfacing the computed dynamic sonar echo returns into the CTFM display consoles.

2. STATEMENT OF THE PROBLEM

To provide a dynamic activation via hybrid computer means, of simulated target data to the displays of a CTFM type sonar so that classification training can be obtained.

3. METHOD OF PROCEDURE

The concept of a computer providing the simulated signals for the CTFM displays is as follows: The digital computer solves those portions of the active sonar equation which contribute measurably to a simulated input to a non-existent transducer. The solution is dependent upon some initial normalized source level and transducer characteristics and the appropriate parameters of sound

transmission and target reflection. This solution will be dynamic, i.e., time dependent. The variation in signal level and noise at the mathematically represented transducer are next fed to a set of analog target generators which "paint" the appropriate picture on the display. Answers to three questions must be provided before simulation can be accomplished:

Section 1. What is the form and content of the active sonar equation and all the associated sonar parameters?

Section 2. What are the electronic techniques in association with programing of a digital computer in order to implement Section (1) and (3)?

Section 3. What are the shapes and moving patterns of the targets displayed in the sonar indicators?

The present report covers Sections 1 and 2. Section 3 will be issued as a separate report in the future.

4. DESCRIPTION OF THE SONAR EQUATION

Extensive investigations have been performed on the transmission of sound in shallow water. Shallow water is usually the environment in which CTFM sonar will be utilized for mine warfare and arctic water navigation, and is customarily defined as that depth less than 100 fathoms. Publications utilized in this portion of the report are references (1) through (10). Appendix A shows additional references and indicates work performed with torpedoes in the arctic region, a subject of interest for the passive mode of the sonars. References (11) - (15) are additional sources of literature for use when applicable.

From reference (5), "The Sonar Equation as conventionally written, is a relation among the various sonar parameters, applicable to the situation in which the probability of detection is 50 percent."

More fundamentally, from reference (9), "The Sonar Equation is a basic equality of system function such that:

"Signal level = background masking level."

Consequently, the above generalized basic equality must now be expanded utilizing the various sonar parameters. The sonar parameters are related to three factors; medium, target, and equipment or platform, as follows:

4.1 Parameters Defined by the Medium

Transmission Loss - TL (dB) [
Ambient Noise Level - NS (dB) [(1)
Reverberation Level - RL (dB) [

4.2 Parameters Defined by the Target

Target Strength - TS (dB) [(2)

4.3 Parameters Defined by the Equipment or Platform

Projector Source Level - LS (dB) [
Self Noise Level - NL (dB) [
Receiving Directivity Index - DI_r (dB) [(3)
Transmitter Directivity Index - DI_t (dB) [
Detection Threshold - DT (dB) [

These and other terms are defined in Reference 1.

4.4 Note on Frequency Dependency

Most of the sonar parameters are frequency dependent. The CTFM sonar, which usually operates in the frequency range greater than 30 kHz, has a large transmitting bandwidth, sometimes on the order of 30 kHz. Consequently, significant differences (i.e., > 3 dB) in values of the sonar parameters can exist between the lower and upper frequencies of the FM sweep. A simplification to this aspect of CTFM is the use of the center frequency of the swept band as the reference point for all frequency dependent sonar parameters. However, if sufficient computer storage is available, either in memory or auxiliary disc, the complete sonar parameter frequency analysis of the swept band can be computed utilizing sufficient frequency increments, so that a less simplified model is used in the simulation. The projector and receiver responses within this bandwidth may not be flat, introducing additional variations. Parameters which are frequency dependent will be indicated in this report and if available in print, the appropriate frequency equation, graph or table will be mentioned for possible future use in the simulation model.

In studying the available literature on shallow water sound propagation it is found that experiments in low frequency, i.e., less than 10 kHz predominate. Additionally, the sonar parameters are empirically determined and reported for frequencies greater than 100 kHz. In the bandwidth between 25 and 80 kHz, which happens to be that of interest for present day CTFM sonars; there is a dearth of experimental evidence.

Also, the low frequency propagation studies are naturally concerned with long ranges involving many reflections from the surface and bottom, whereas, the CTFM sonar environment for downward refraction would be concerned primarily with either the two way direct ray path (RBR) or the two way bottom surface reflected (BSR) ray path to the target and back (or its limiting ray path which may not touch the sea surface). See Figure 1. Consequently, the water thermal structure surrounding the sonar platform will determine the particular ray path geometry, and must of course form part of this simulation model. This is discussed in more detail later.

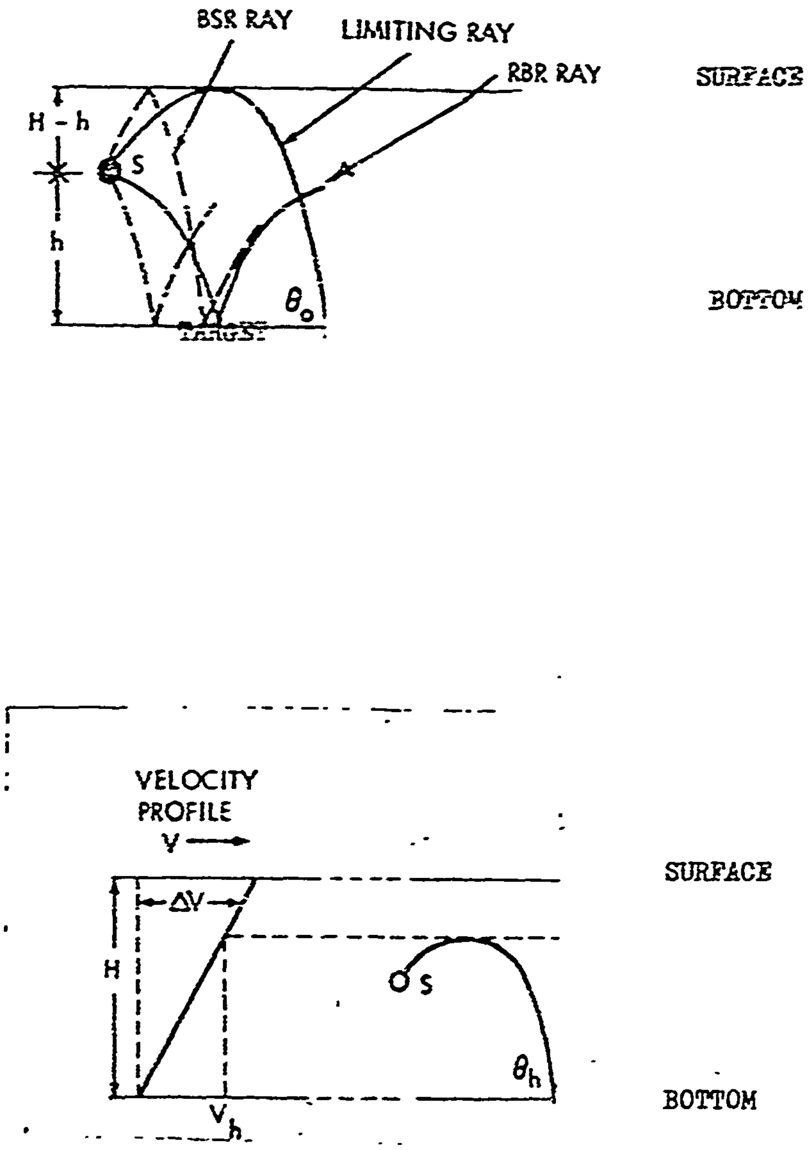

FIGURE 1. Typical ray diagrams for the shallow water minefield environment

4.5 Note on Background Masking Level

The background masking level will consist of both noise and reverberation. Usually in the shallow water sonar environment, the predominating background level for the active case, will be composed of reverberation. However, if the water is sufficiently deep and the projected sound rays are at shallow angles with respect to the bottom and surface, the self and/or background noise can predominate. Thus, as a function of increased range, the echo level falls off more rapidly than the reverberation level, so that, unless the noise masking level is high, the reverberation level will predominate.

In discussing the sonar equation in the following pages, the two background masking level type equations are shown, i.e., the noise limited equation and the reverberation limited. For purposes of simulation, both equations should be utilized and preferably during the conduct of a training session, whereby the sonar carrying vehicle can enter a noise limiting environment from a reverberation environment or vice versa.

5. NOISE-LIMITED ACTIVE SONAR EQUATION

From references (3) and (10) the sonar equation of the noise limited environment for active sonar is:

Signal Level - Background Masking Level = Excess Signal = ES (dB)
or $ES = TS - [(TL) - LS - DI_r + NS]$ (4)

5.1 Ambient Noise - NS

An example of a typical background noise spectra (NS) is shown in Figure (1) of reference (3). Reference (10) also contains graphs of typical ambient noise situations. An examination of Figure (1) in reference (3) shows that in the region of 20 kHz to 80 kHz, the ambient noise decreases 5 dB per octave from a maximum of approximately - 42 dB/dyne/cm^2 at the upper limit of prevailing noise and 20 kHz. These values are also shown in reference (10), figures 7.5 and 7.7. Reference (10) shows additional curves of ambient noise for sea animals and rain in various locations. The data shown in Figure (1) of reference (3), for example, can be stored in tabular form of spectrum level versus frequency for the various traffic conditions, or equations can be fitted to the curves shown. If in the development of the CTFM trainer, specific inshore area ambient noise levels are deemed necessary, a literature search for values in that area should be made, or a sound survey performed. Reference (5), page 294, lists a formula covering the Knudsen curves of ambient noise. Here there is already available the means for computing typical ambient values.

5.2 Receiver Directivity Index - DI_r

This parameter is a measure of how the receiving hydrophone by virtue of its directional response (i.e., beam pattern) detects the signal in a noisy environment. In order to evaluate the directivity index, measurements of the beam pattern are utilized. Reference (1) indicates that the directivity index can be expressed as:

$$DI = 45.9 - 20 \log \theta \text{ (dB)}$$

where θ is total horizontal angular beamwidth in degrees at the 3 dB points below the maximum response. Assuming the horizontal angular beamwidth is on the order of 5 degrees, which approximates the value found in CTFM sonars operating between 20 kHz and 90 kHz, it is computed from the formula above, that DI_r = 32 dB. This value is in the range of interest for the simulation model.

5.3 Projector Directivity Index - DI_t

The Projector Directivity Index is defined as ten times the log of the ratio of the directional sound intensity along the main beam axis, to the non-directional intensity. The beamwidth is related to the size of the projector and the transmitting frequency.

5.4 Source Level - LS

This parameter was needed previously for determining the Projector Directivity Index. This value will vary with each sonar system and its operating condition. A typical peak performance value is approximately 100 dB.

Further refining relates it to the source level and acoustic power output, reference (10), as:

$$LS = 71.5 + 10 \text{ Log } P + DI_T \text{ (dB)} \qquad (5)$$

where P is the acoustic power output. Hence:

$$DI_T = LS - 71.5 - 10 \log P. \qquad (6)$$

A typical value of DI_T for a CTFM would be obtained by having

LS = 100 dB (typical peak performance value)

so that under these circumstances

$$DI_T = 29.5 - 10 \log P. \text{ (see Figure 4)} \qquad (7)$$

5.5 Transmission Loss - TL

This parameter is the more significant and contains numerous environmental phenomena contributing to the loss. Contributing factors are:

1. Thermal gradients
2. Bottom or sea floor reflections
3. Surface reflections
4. Spreading loss
5. Acoustic energy absorption
6. Phase interferences
7. Internal waves
8. Volume scattering and reverberation

Some of the above phenomenon are inter-related, i.e., internal waves affecting the thermal gradients.

5.6 Thermal Gradients

The presence of the thermoclines in shallow water affects sonar performance at mine hunting frequencies, reference (11). Its effect in transmission loss exists by virtue of the bending of the sound rays so that decreased sound energy reaches the target area.

5.7 Bottom Losses

5.7.1 Reflection Loss

Reference (12) represents an existing computer program giving emperical values for the bottom reflection loss. The expression for bottom reflection loss in dB per bounce is a function of the porosity of the bottom, frequency in kHz and bottom grazing angle in degrees. The equation of reference (12) is not sensitive to frequency variation at the bandwidth of interest for CTFM, providing the expression can be extrapolated up to this value. Twelve separate bottom composition types can be utilized in the program, so that a wide variety of minefield areas can be programed.

Reference (10), page 118, shows a graph and table of bottom loss for frequencies of interest to CTFM. If the above, reference (12) values are not applicable, then the curves from reference (10) can be used to stipulate the bottom loss. This loss is subtracted from equation (4) when the path to and from the target is via a bottom bounce.

5.8 Surface Losses

5.8.1 Reflection Loss

Reference (10), page 128, shows a graph of surface loss/bounce versus frequency times wave height. This curve is very easily programable, and can be utilized for this portion of the sonar equation. This loss is subtracted from equation (4) when the path to and from the target is via a surface bounce.

5.9 Spreading Loss

This loss is the weakening of the sound intensity by virtue of a geometric effect in spreading the acoustic energy over larger and larger surfaces.

In a free field, the spreading loss would be 20 log (range), so-called spherical spreading, and in a shallow water environment, at large ranges from the source, the spreading loss would be 10 log (range), so-called cylindrical spreading. In the shallow water environmental range of the CTFM sonar, which is a maximum of 3000 yards, neither one of the above laws would be completely applicable. The variation between observed spreading losses and predicted spherical or cylindrical spreading has been called the transmission anomaly, reference (7). This transmission anomaly is dependent on the sonar location, frequency and the medium.

Consequently, the one-way spreading loss is defined as a function of spherical spreading and a correction term:

$$L_S = 20 \log r + \alpha r \qquad (8)$$

where

r = range

α = attenuation in decibles/yard.

For isothermal conditions, (in the arctic regions for example), the attenuation factor is primarily due to absorption. For other thermal conditions, the attenuation constant is primarily dependent upon refractive effects. This loss is subtracted twice from equation (4).

Reference (7), figure 4.6, shows a typical graph of transmission anomaly (αr) in dB versus range. This kind of graph can very easily be programed for use.

5.10 Acoustic Energy Absorption

This loss due to absorption is enclosed in the attenuation coefficient, α, for the spreading loss case. For the absorption only situation, Figure 3.2 of reference (7), shows the value of this parameter.

5.11 Phase Interference

This phenomena would cause fluctuations in the sound pressure level received at the hydrophone. Although this occurrence is very difficult to predict when echo ranging, its effect can still be implemented during the simulation process. Attenuation circuits within the simulator can be programmed at statistical intervals to provide the necessary fluctuations to the computed signal levels.

5.12 Internal Waves

Internal waves cause changes in the thermocline temperature distribution. As a result, sound pressure levels will fluctuate at the receiver. The effect on the sonar displays will be identical to the above phase interference effect. Consequently, the attenuation circuitry previously indicated for the phase interference phenomena, will be applicable for this effect.

5.13 Volume Scattering and Reverberation

From Reference (7), this phenomena is shown to be represented as part of the attenuation coefficient, α, of the spreading loss expression.

6. SUMMARY OF TRANSMISSION LOSS

The total loss then consists of any possible combination of the above factors, i.e., the paths as shown in Figure 1. Note particularly that if the total path is from source to target and then return to receiver along the same path, that the loss is twice the one-way path.

7. TARGET STRENGTH

The targets of primary interest in CTFM training would be as follows:

a. Suspended mines

b. Bottom Mines

c. Bottom Mine-like Objects

d. Bottom Non-Mine Objects

e. Surface Vessels and Submarines

f. Polar Ice Cover and Polynya

g. Bottom Features in Estuaries and Harbor Entrances.

Much of the information concerning the values of target strength is either classified or undetermined. However, sufficient unclassified information exists to describe certain of these targets in this report. The simulator model will have to obtain a more widespread amount of information for use in training.

For a spherical suspended mine, whose diameter is approximately 30 inches, its target strength (independent of frequency) can be found directly from reference (7), Figure 4.7, "target strength of a sphere as a function of diameter."

The value comes out to be approximately -14 dB. (Target strength is defined in Reference 1).

Reference (8) discusses the target strength of bottom mines. However, because of the classified nature of these values they will not be listed.

The target strengths of bottom mine-like and non-mine objects can be computed from reference (10), Table 9.1. In this table, numerous geometric shapes are shown under various conditions of aspect, with formulas for target strength listed. All of these values are programable. Reference (10) also refers to Table 9.1 as being applicable to mine target strengths, and also shows some typical values of mine target strengths in Table 9.2.

The scattering strength of polar ice is shown in reference (10), Figure 8.28. However, the frequency range is far below CTFM sonars. Information on polar ice and bottom features scattering strength can be obtained from the Naval Undersea Research and Development Center at San Diego.

8. REVERBERATION-LIMITED ACTIVE SONAR EQUATION

From references (3) and (10), the sonar equation of the reverberation limited environment for active sonar is:

Signal level - Background reverberation level = excess signal,

or

$$ES = TS - (2\ (TL) - LS + RL) = T_S - T_{bs} \qquad (9)$$

where: $R_L = LS + T_{bs} - 2\ TL$ and T_{bs} is defined below.

Comparing equation (4), the noise-limited equation with equation (9) above, it is seen that the noise level and directivity parameters are replaced with the reverberation level, RL. Other parameters remain the same.

The major contributor to the reverberation level is the bottom and/or surface reverberation.

8.1 BOTTOM AND SURFACE REVERBERATION

Reference (3) has information on bottom reverberation, defined as:

$$T_{bs} = S_b + 10 \log \psi + 10 \log \Delta R + 10 \text{ Log } r \qquad (10)$$

where T_{bs} = Background Reverberation Level

S_b = reflected-to-incident-intensity ratio, which is a function of grazing angle in degrees and for which a typical plot is shown in reference (3).

R = Horizontal range in yards to the target on which echo ranging is being performed.

ψ = Horizontal directivity of the receiving hydrophone, radians

ΔR = Range internal from which reverberation is received and which is determined by the filter bandwidth and range scale use.

8.2 VOLUME SCATTERING AND REVERBERATION

Volume reverberation can be defined as the volume scattering strength per unit volume. The preponderant source of volume scattering is the so-called Deep-Scattering Layer, which is absent in shallow water. Reference (3), recognizing that insufficient data on this effect exists in shallow water, has shown a frequency independent curve. (See reference (3), Figure 11 for volume scattering strength versus water depth.) This curve can easily be programed for use.

9. SUMMARY

Figures 2, 3 and 4 (obtained from Mr. Garland Bernard of the Applied Research Laboratory of the University of Texas) summarizes in graphical form the interdependence of the parameters entering into both the sonar equation and the sonar equipment, reference (16).

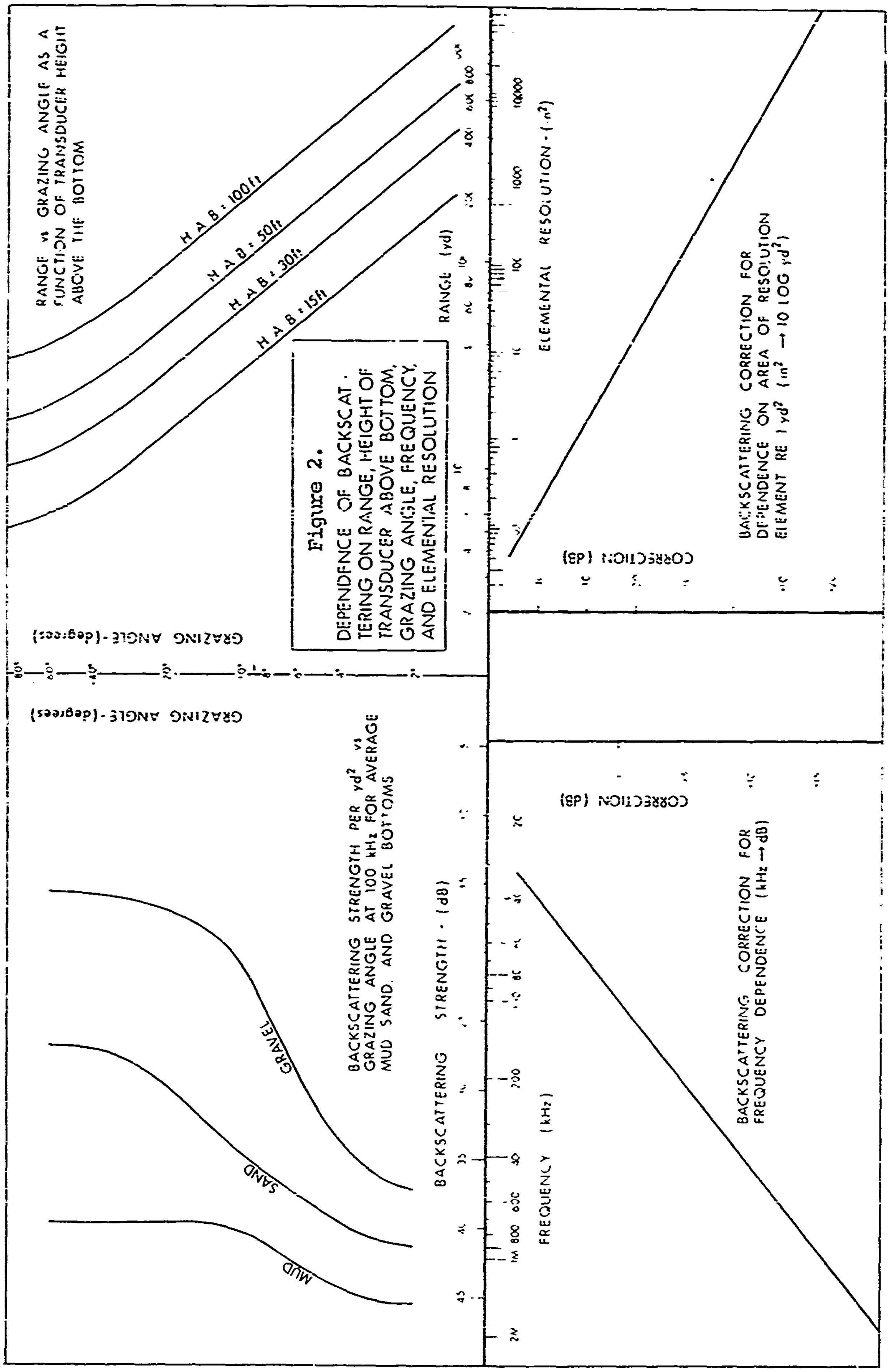

Figure 2.
DEPENDENCE OF BACKSCATTERING ON RANGE, HEIGHT OF TRANSDUCER ABOVE BOTTOM, GRAZING ANGLE, FREQUENCY, AND ELEMENTAL RESOLUTION

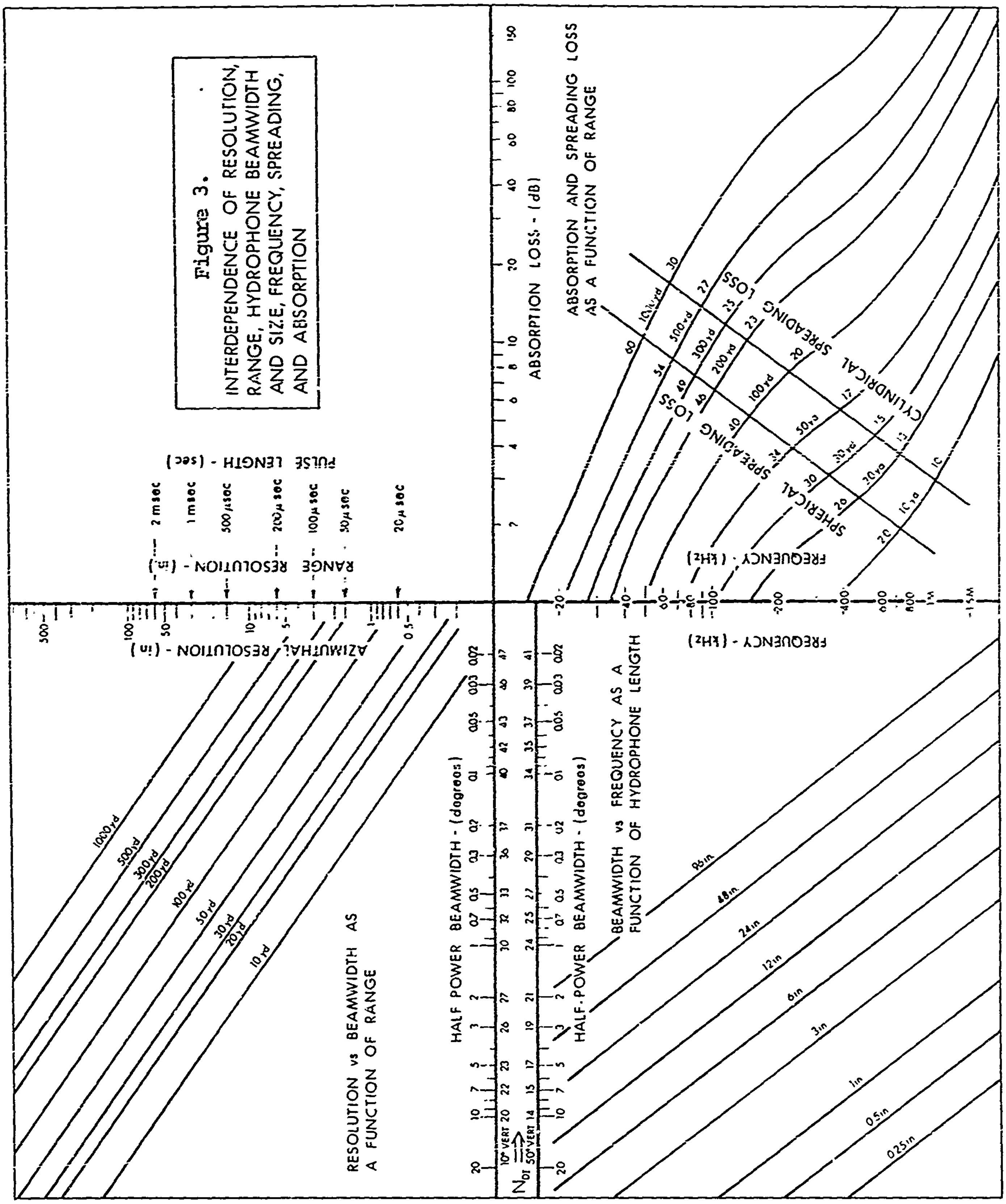

Figure 3.
INTERDEPENDENCE OF RESOLUTION, RANGE, HYDROPHONE BEAMWIDTH AND SIZE, FREQUENCY, SPREADING, AND ABSORPTION

DRL - UT
DWG CS 66 458
TGM OPS
6 - 9 - 66

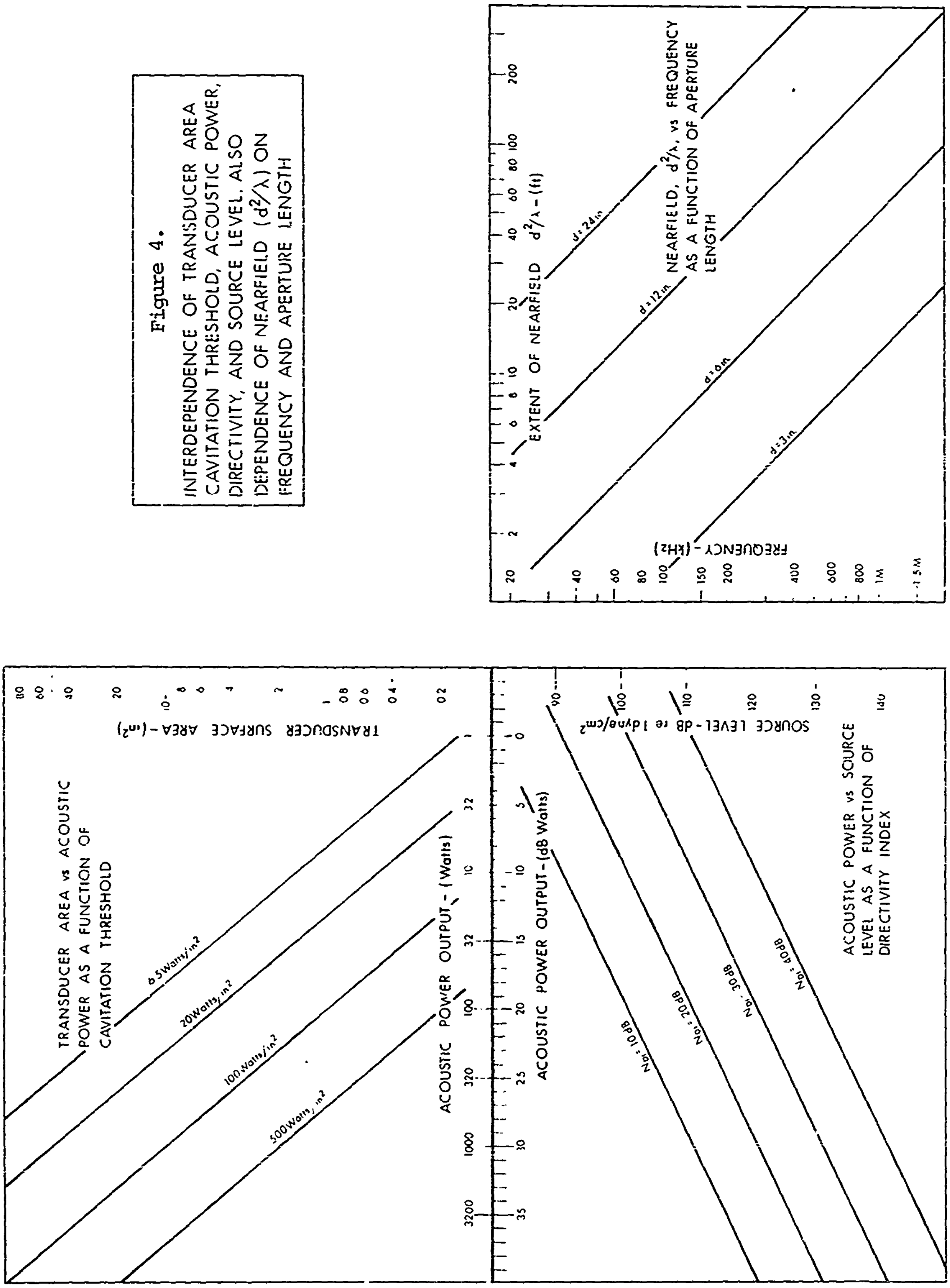

Figure 4.

INTERDEPENDENCE OF TRANSDUCER AREA CAVITATION THRESHOLD, ACOUSTIC POWER, DIRECTIVITY, AND SOURCE LEVEL. ALSO DEPENDENCE OF NEARFIELD (d^2/λ) ON FREQUENCY AND APERTURE LENGTH

DRL - UT
DWG CS-66-459
TGM - ORS
6 - 10 - 66

REFERENCES

1. Summary Technical Report of Division 6, NDRC, "Frequency Modulated Sonar Systems", Washington, D.C., 1946

2. Underwater Systems, Inc., "A Review and Summary of Shallow Water Propagation Research (1955-1968)", Silver Spring, Maryland, 1969

3. Operations Research, Inc., "A Prediction Model for the Performance of Sonars in Shallow Water", Silver Spring, Maryland, 1967

4. Naval Undersea Warfare Center, "Shallow Water Propagation Loss Model (1)", San Diego, California, 1967.

5. Bartberger, C.L., et al., "Lecture Notes on Underwater Acoustics", Johnsville, Pennsylvania 1965 (AD 468869)

6. Officer, C.B., "Introduction to the Theory of Sound Transmission", New York, McGraw-Hill, 1958

7. Albers, V.M., "Underwater Acoustics Handbook - II", University Park, Pennsylvania, The Pennsylvania State University Press, 1965

8. C. M. McKinney, et al., "Mine Classification with High Resolution FM Sonar, Parts I, II, III", Austin, Texas, 19?9 (Confidential)

9. Catholic University of America, "Acoustics Notes", Washington, D. C., 1968

10. Urick, R.J. "Principles of Underwater Sound for Engineers", New York, McGraw-Hill, 1967

11. Technical Development Plan (TDP) S26-10, Submarine Mine Detection, Close Contact and Avoidance Sonar, NAVSHIPSCOM, Washington, D.C. (Confidential)

12. Naval Undersea Warfare Center, "An Empirical Bottom Reflection Loss Expression for use in Sonar Range Prediction", San Diego, California, 1967

13. Mine Advisory Committee, National Academy of Sciencies - National Research Council, "High Resolution Sonar Technology (U), Volumes 1 and 2, Washington, D.C., March 1969 (CONFIDENTIAL)

14. J. F. Wilkinson, "Summary Report. Reformulation of the Sonar Equation, Part 1", TRACOR, Austin, Texas, July 1966

15. R. J. Urick and A. W. Pryce, "A Summary of Underwater Acoustic Data", ONR, Washington, D. C., 1953

16. T. G. Muir, "Basic Acoustic Minehunting", Applied Research Laboratory, University of Texas, Austin, Texas, DRL-A-264, 1966.

APPENDIX A

LIST OF REFERENCES - SHALLOW WATER PROPAGATION

1. Normal Mode Theory Applied to Short Range Propagation in an Underwater Acoustic Surface Duct, M. A. Pedersen and D. F. Gordon, J.A.S.A. 37, No. 1, January 1965, p. 105. 530 to 1030 cps. 10 kyd.

2. Shallow Water Transmission, H. W. Marsh and M. Schulkin, J.A.S.A. 34, 863-864, 1962. Transmission loss as a function of bottom type, sea state, frequency, water depth and range. 1 to 10 kc., 3 to 90 kyd.

3. New Models for Shallow Water Propagation, H. P. Bucker and H. E. Morris, NUWC TN-45, January 1968. Several shallow water normal mode models Epstein velocity profile, etc. 115 to 135 yds depth, 1.5 kc 0-50 kyd.

4. Epstein Normal Mode Model of a Surface Duct, H. P. Bucker and H. E. Morris, J.A.S.A. 41, No.6, p. 1475. 0 to 10 kyd., 1030 Hz.

5. Normal Mode Surface Channel Propagation Loss, USNEL. USNEL (Code 3185 Model and Code 3110D Model). 10 year research effort by NEL. 50 cps to 30 kc.

6. A.S.W. Sonar Technology Report Shallow Water Acoustics, A. D. Little November 1967, 148 pp. Report No. 4241167.

7. A Handbook of A.S.W. Computer Models, Vol. I and Vol. II. Prepared by NOTS and NEL, March 1967, S.A.G. Report 67-4. Systems Analysis Group NOL, 83 programs, 20 on acoustic propagation.

8. The Propagation of Sound in Imperfect Ocean Surface Ducts, M. Schulkin, 22 April 1969, USL Report No. 1013, 128 pp.

9. Analysis of Spreading Loss for Refracted/Reflected Rays in Constant-Velocity-Gradient Media, M. J. Jacobson, J.A.S.A. 36, No. 12, December 1964. Spreading loss for refracted/bottom reflected rays when the velocity gradient is a negative constant and the bottom is horizontal.

10. Analysis of Surface-Reflected/Bottom-Reflected Ray Transmissions in Constant-Velocity-Gradient Media, M. J. Jacobson, J.A.S.A. 37, No. 5, May 1965. Horizontal surface and bottom sound velocity either positive or negative.

11. Ray Transmissions in an Underwater Acoustic Duct with a Pseudorandom Bottom, A. D. Seifer and M. J. Jacobson, J.A.S.A. 43, No. 6, 1968, p.1395. Isovelocity sound channel bounded by a lossy pseudorandom facet bottom below and a free, planar surface above.

12. Refracted/Reflected Ray Transmissions in a Divergent Channel, M. J. Jacobson, J. G. Clark, J.A.S.A. 41, No. 1, 1967, p. 167. Sound velocity decreases linearly with depth.

APPENDIX A (continued)

List of References Continued

13. Ray Transmissions in an Underwater Acoustic Duct with a Bottom Having Curvature, A. D. Seifer and M. J. Jacobson, J.A.S.A. 44, No. 4, 1968, p. 1103. A general spreading loss expression bottom loss.

14. Surface-Reflected/Bottom-Reflected Ray Transmissions in a Divergent Channel, M. J. Jacobson and J. T. Warfield, J.A.S.A. 43, No. 1, 1968, p. 15.

15. Practical Model of Shallow Water Acoustic Propagation, J. D. Macpherson and M. J. Dainteth. J.A.S.A. 41, No. 4, 1967, p. 850. Water depth, bottom slope, reflection losses and velocity gradients in the water are taken into consideration.

16. Intensity-Decay Laws for Sound Propagation in Shallow Water of Variable Depth., R. N. Denham, J.A.S.A. 39, No. 6, 1966, p. 1170. Normal mode theory.

SECTION II

A MEANS OF SIMULATING TARGET ECHOS ON THE DISPLAYS OF THE CONTINUOUS TRANSMISSION FREQUENCY MODULATED SONAR

By: FRANCIS MURPHREE

1. INTRODUCTION

This report outlines a proposed means for simulating the performance of a CTFM sonar to the extent that the simulated signal will sound realistic and will appear realistic on the CRT display.

2. BACKGROUND

A CTFM sonar consists of the following:

a. An exciter which generates a frequency modulated wave changing linearly with time as suggested by Figure 1. The extent of the total frequency change is on the order of 10 to 15 kHz; the time required to complete a cycle is typically 2 to 5 seconds. The rate of change $\frac{df}{dt}$ equals the total change divided by the time required to complete this change.

b. A power amplifier driven by the exciter.

c. A projector having a horizontal beamwidth of from 30° to 180° driven by the power amplifier.

d. A narrow beam (2° to 5°) receiving hydrophone that scans the sector illuminated by the projector.

e. A receiver having a mixer in which a sample of the signal fed to the projector is beat with the echoes received by the hydrophone. The difference frequency output of the mixer lies in the audible region so that the range to a target can be estimated by the pitch of its echo. The frequency response of the receiver rises at the rate of 9 to 12 dB per octave to approximately compensate for the increased loss suffered by echoes with increasing range.

f. A bank of from 30 to 50 range measuring filters driven by the receiver. Each filter usually has a bandwidth of about 50 cycles; the range of frequencies covered is from about 500 Hertz to 2000 Hertz.

g. A PPI or B scan CRT display and associated circuitry.

h. An audio system covering the entire Frequency band analyzed by the range filers.

Assume that a fixed, point target is at a range R and azimuth Θ relative to a stationary CTFM sonar. Under these conditions each time the receiving

hydrophone scans past the target an echo of frequency $F = \frac{2R}{C}\frac{df}{dt}$ will be heard on the loudspeaker and displayed on the CRT, where C is the velocity of sound in water and $\frac{df}{dt} = k$ is the rate in cycles per second at which the transmitted frequency is being changed. Thus if $\frac{2R}{C} = 1$ second and $\frac{df}{dt} = 1000$ cycles per second per second, $f = 1 \times 1000 = 1000$ cycles/sec. A target twice as distant would return an echo of 2,000 cycles per second; one half as far would return an echo of 500 cycles/sec. The range scale is changed by increasing or decreasing $\frac{df}{dt}$ so that a given frequency does not correspond to a single range.

If relative motion exists between the sonar platform and the target the echo frequency $f \approx \frac{2R}{C}\frac{df}{dt} + .7\dot{R}f_0$, where $\dot{R}$ is the range rate in knots between the sonar and the target and f_0 is the mean transmitted frequency. If the target is stationary $f \approx \frac{2R}{C}\frac{df}{dt} + .7v \cos\theta\, f_0$, where v is the velocity of the sonar platform and θ is the angle between the velocity vector and the direction to the target.

The duration of the echo (assuming a point target) is $\tau = \frac{\Phi}{\omega}$ seconds where Φ is the receiving beamwidth and ω is the rate at which the hydrophone is scanned in azimuth. If, for example, $\Phi = 5°$ and ω is 30° per sec, then $\tau = \frac{5}{30} = .166$ sec.

In addition to the target echo, reverberation caused by sound scattered from the bottom, surface and volume of the water may be heard from all ranges and bearings and will show to some extent on the CRT. Ambient, own ship and target noise may also be present.

A phenomena exhibited by CTFM sonars is that of "lost time." It is caused by the fact that immediately after the modulating sawtooth returns to its starting point the difference between the frequency being transmitted and that being returned from a target or scatterer is too great to pass through the receiver filters, as suggested by Figure 1. "Lost time" lasts for $\frac{2R}{C}$ seconds; i.e., the time required for the sound to propagate to a range R and to return. For example, if the hydrophone was pointed at a target 800 yards distant from which an echo was being received, at the instant the sawtooth returned to its starting point the echo would apparently cease for one second. (Nearer targets would cease for shorter intervals). The echo would then be heard until "fly back" again occurred and the cycle repeated.

3. Proposed CTFM Simulator -

Referring to the block diagram, Figure 2, the phenomena discussed above can be simulated as follows. A programable oscillator 1 is adjusted to a frequency f equal to that which would be generated by a moving or stationary target at a range r by means of a signal from an external computer 2. The output of azimuth function generator 3 causes the CRT beam to sweep over the scope face corresponding to the changes in direction in which the receiving hydrophone points. When the direction of the hydrophone (and position of the beam) agrees with the azimuth at which a target is to appear, Gate 22 is turned on by a signal from generator 3, feeding a signal from the programable oscillator through azimuth attenuator 4, gain adjustment 5 and summing network 6. The azimuth attenuator changes the level of the oscillator output as the azimuth changes in the same manner as the echo would change when the receiving hydrophone scans past the target. The gain adjustment 5 changes the average intensity of the simulated echo and may be adjusted manually or automatically.

The output of the summing network 6, is applied to "lost time" gates 9 and 10, summing networks 23 and 24 and thence to bandpass filters 7 and 8 (in a complete system 30 to 50 filters and gates would be used). Each filter passes a band of frequencies corresponding to a range interval Δr. Detectors 11 and 12 rectify the filter outputs. The detectors are scanned sequentially (in a conventional manner) by detector sampler 13. Sufficiently strong signals appear on CRT 14. The detector scanning rate and the CRT vertical deflection rate are synchronized so that a signal (such as the output of the programable oscillator in the present case) that lies within the pass band of a given filter will cause an intensity modulated spot to appear at the same CRT range each vertical scan.

One output of the azimuth function generator is applied to the CRT horizontal deflection input, causing the beam to move across the face of the tube; the target appears at the ordered azimuth over a sector corresponding to the receiving beamwidth. (It is assumed for this discussion that a "B" scope display is used).

Also appearing on the face of the CRT will be signals caused by the reverberation noise generator 15 whose output is applied to gain adjustment 16, to range filter 25 and to summing network 6 which connects to the remainder of the pertinent circuitry. The reverberation generator is a wide band source and causes an interferring signal to appear on each channel with an intensity depending upon the adjustment of gain control 16 and the reverberation spectrum as determined by filter 25.

Several factors influence the design of the simulator at this point. Both desired echoes and reverberation become weaker with increasing range in the real world situation. In an attempt to compensate for this fact CTFM receivers are designed to have a progressively greater response with increasing frequency, commonly at the rate of 9 to 12 dB per octave; for example,

the response at 2000 Hz may be 24 dB greater than at 500 Hz. The compensation is not necessarily perfect, however. Detected noise, unlike reverberation, is fairly uniform over the same frequency range so that the effect of the increased high frequency amplification is to make the noise appear to be much stronger at the higher frequencies.

This total effect may be simulated in several ways. In Figure 2 the effect of less than perfect reverberation compensation is introduced by sloping off the reverberation by filter 25. Own ship, ambient and target noise is fed through a range compensation network 26 that raises the high frequency components at the same rate as is normally accomplished in the receiver so that for similar relative levels of noise and reverberation the simulated display will closely resemble an operational display.

Ambient, own ship and target noise is inserted as shown to prevent it from passing through the "lost time" gates. "Lost time" applies only to target echoes and reverberation. The azimuth attenuator 27 is used to cause the target noise to change in intensity as the simulated beam sweeps across the target; the "target" can be a noise source other than the one returning the echo.

In addition to being applied as signal voltages to the CRT, the simulated reverberation noise and signal are applied via summing network 19 and gain control 20 to the amplifier loudspeaker combination 21 and 28.

4. Lost Time Function (Figure 4)- Lost time gates 9 and 10, Figure 2, are normally "on". When the range time base generator 17 recycles the lost time function generator 18 turns all gates "off". They are then progressively turned back on, each at a time = $\frac{2R}{C}$ seconds after the recycle or "flyback", where R is the range corresponding to the frequency of the filter to which a particular gate is connected. Since the range corresponding to a given frequency f is not unique but depends upon the range scale and hence the value of $\frac{df}{dt}$ to which the set is adjusted, the lost time function must change with changes in the range scale. Figure 3 demonstrates this.

Figure 4 shows in block diagram form one arrangement for accomplishing the lost time function. Figure 5 is the timing diagram corresponding to Figure 4. When the range time base 17, Figure 2, recycles as shown on line a, Figure 5, flip-flop 5, Figure 4, changes state and turns on oscillator 6, feeding a signal through $\div$ n circuit 7 to counter 8. Simultaneously, FF1 and FF2 are also triggered on closing lost time gates 9 and 10, Figure 2. These gates stay off (closed) until triggered back on by a pulse from counter 8. The time elapsing between turn off and turn on is determined by the frequency f_0 of the oscillator 6 and by n, the quantity by which f_0 is divided before being applied to the counter. In this discussion lost time gate 10 is assumed

to be connected to the maximum range filter; when this gate is turned back on by the last counter pulse, the counter, the divide by n circuit, and FF5 are all reset to their original state by the same pulse. The circuit is then ready to repeat the cycle. When the range scale is changed f_0 must be changed also; i.e., if the maximum range is halved, f_0 must be doubled, and so on).

5. Azimuth Function Generator (Figure 6) - One arrangement for the azimuth function generator is shown in Figure 6. A reversible motor 1 is used to drive a potentiometer 2. The voltage across the arm of the potentiometer is triangular as shown in Figure 7. This triangular voltage waveform is used to deflect the CRT beam horizontally and is also compared with computer generated azimuth reference voltages to generate gates that turn on the programable oscillator at the desired azimuth.

As shown in Figure 6, the potentiometer arm is connected to the inputs of azimuth comparators 3 and 4. The reference voltage applied to 4 is derived from a D/A converter 15 which changes a digital number corresponding to an azimuth command (the target appears at this azimuth) to a d.c. voltage. This voltage attenuated by resistance networks R_1 R_2 is used also as the reference for comparator 3.

Assume that the voltage across the potentiometer arm is initially lower than the trigger levels a, b of comparators 3 and 4 and that it begins to increase. As it crosses the reference level of comparator 4 (point a) this last generates a pulse that is applied through gate 8 to the set input of FF11 (assumed to have been "off" previously). A logical "one" appears at the output of FF11 and turns on gate 22, Figure 2. As the voltage continues to increase it crosses the reference of azimuth comparator 3 (point b). The resultant trigger pulse is applied through gate 7 to the reset input of FF11 turning it "off" and hence closing gate 22, Figure 2. As the potentiometer continues to rotate the voltage across its arm rises to some maximum value. At this point (or for any greater voltage) the high limit comparator 5 triggers applying a signal to the reset terminal R of FF12 changing its output to zero and hence closing gates 7 and 8. This action also causes the polarity of the voltage applied to the motor 1 to reverse via motor reversing circuit 13 making the motor rotate in the opposite direction. The voltage across the potentiometer arm then begins to decrease. When it reaches point c, Figure 7, azimuth comparator 3 triggers and through gate 9 applies a pulse to the "set" input of FF11. This turns on gate 22, Figure 2, as before. When the voltage reaches point d azimuth comparator 4 operates, applies a pulse through gate 10 to the reset of FF11, shutting off gate 22. As the potentiometer rotation continues the voltage across its arm reaches a value below which the low limit comparator 6 triggers and applies a signal to the set input of FF12. This causes a 1 to appear at its output which reverses the direction of the motor and opens gates 7 and 8. Gates 9 and 10 are closed. These actions set up the same sequence of events as before.

The R_3 C_1 - switch combination 14 makes it possible to reset FF11 to "off" if by chance it starts in the "on" position when power is first applied.

Usually there would be more than one target, or a given target may consist of a number of distinct highlights so that the computer must be programed to handle this problem. In addition, use of more than one programed oscillator will be necessary whenever the problem results in more than one target within a given bearing sector.

6. <u>Azimuth Attenuator (Figure 8a)</u> - The azimuth gate signal from the azimuth function generator turns on a gate 2 (Figure 8a) connecting a clock 1 to pulse generator 3 and thence to counter 4. Successive clock pulses cause FETS (1) through (5) to be sequentially turned on allowing smaller or larger signals from the programable oscillator to appear across the output resistor R_0 depending upon the relative value of the resistors R_1 through R_5 in the dividing network. A possible amplitude sequence is shown in Figure 8b. It is evident that as many steps as desired may be employed to approximate any desired target-beam response curve.

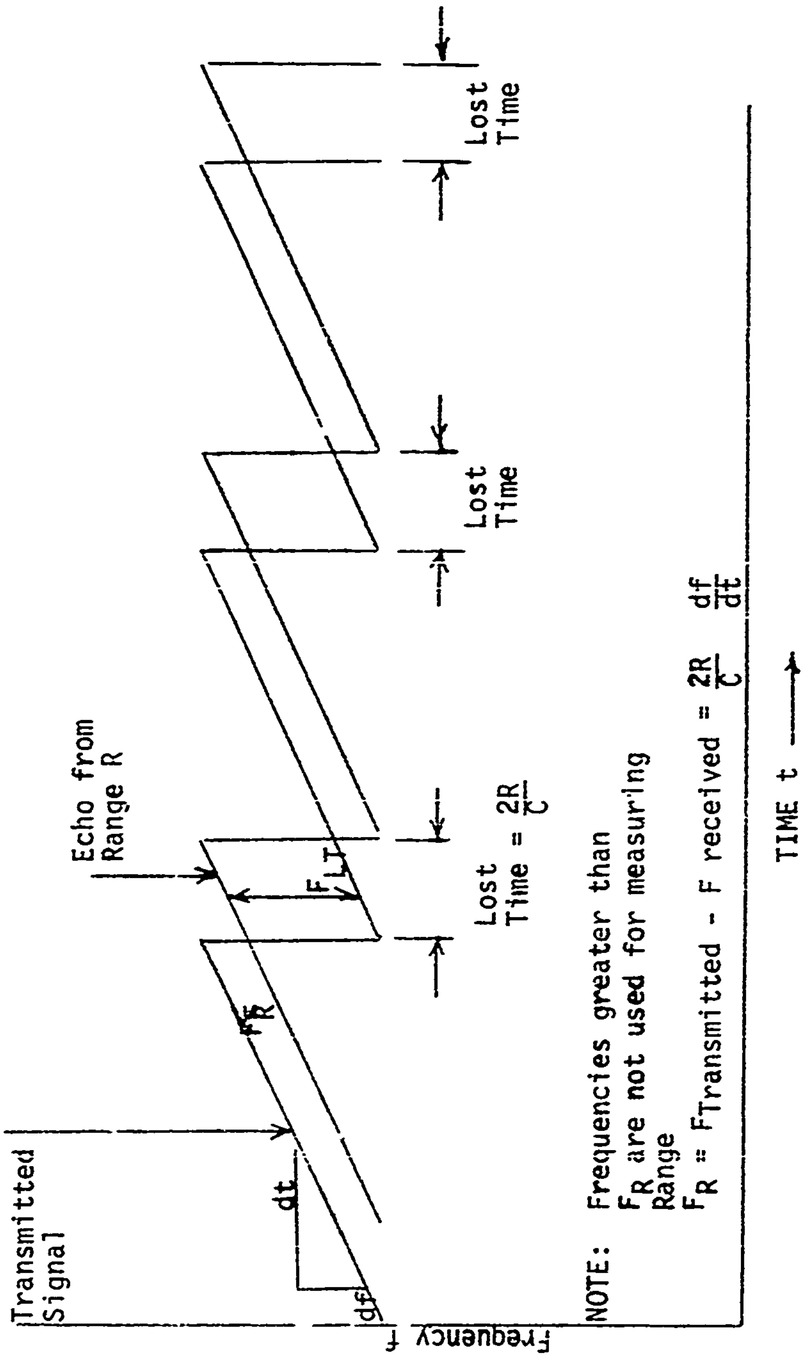

Figure 1.

Sketch showing relation between transmitted and maximum range received signal for CTFM Sonar

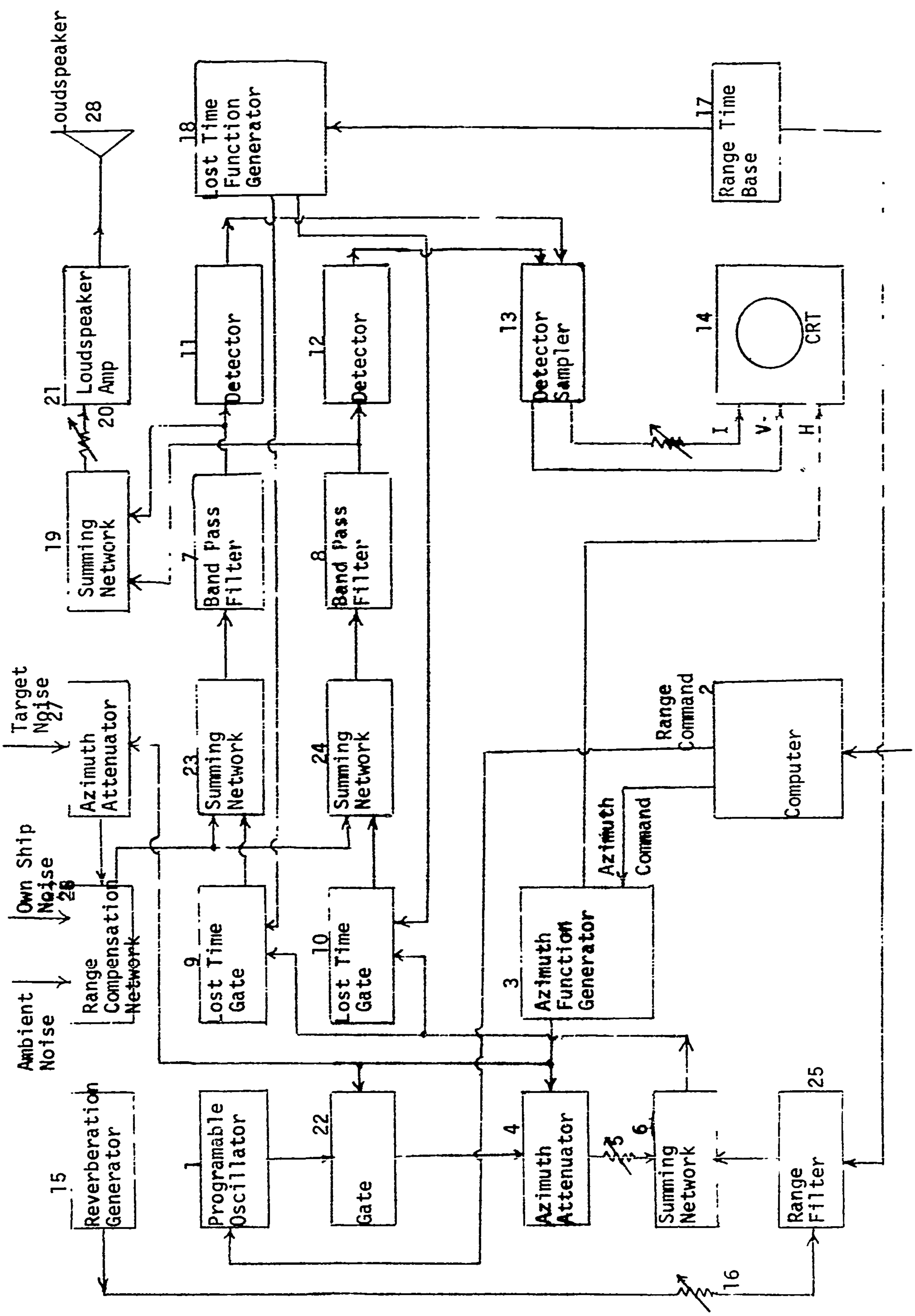

Figure 2.
OVERALL BLOCK DIAGRAM

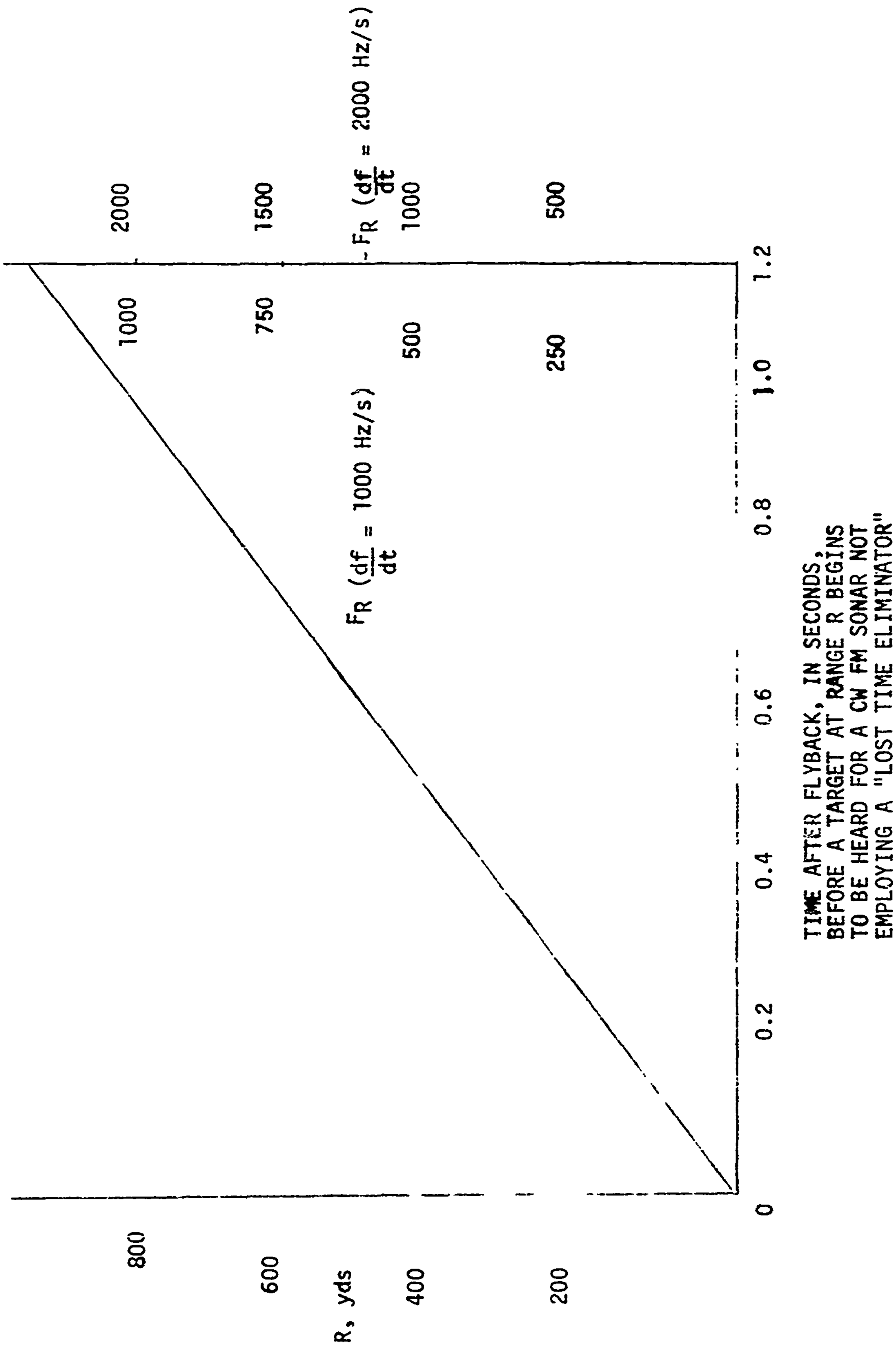
F_R ($\frac{df}{dt}$ = 2000 Hz/s)
2000
1500
1000
500
F_R ($\frac{df}{dt}$ = 1000 Hz/s)
1000
750
500
250
R, yds
800
600
400
200
0
0.2
0.4
0.6
0.8
1.0
1.2
TIME AFTER FLYBACK, IN SECONDS,
BEFORE A TARGET AT RANGE R BEGINS
TO BE HEARD FOR A CW FM SONAR NOT
EMPLOYING A "LOST TIME ELIMINATOR"

Figure 3.

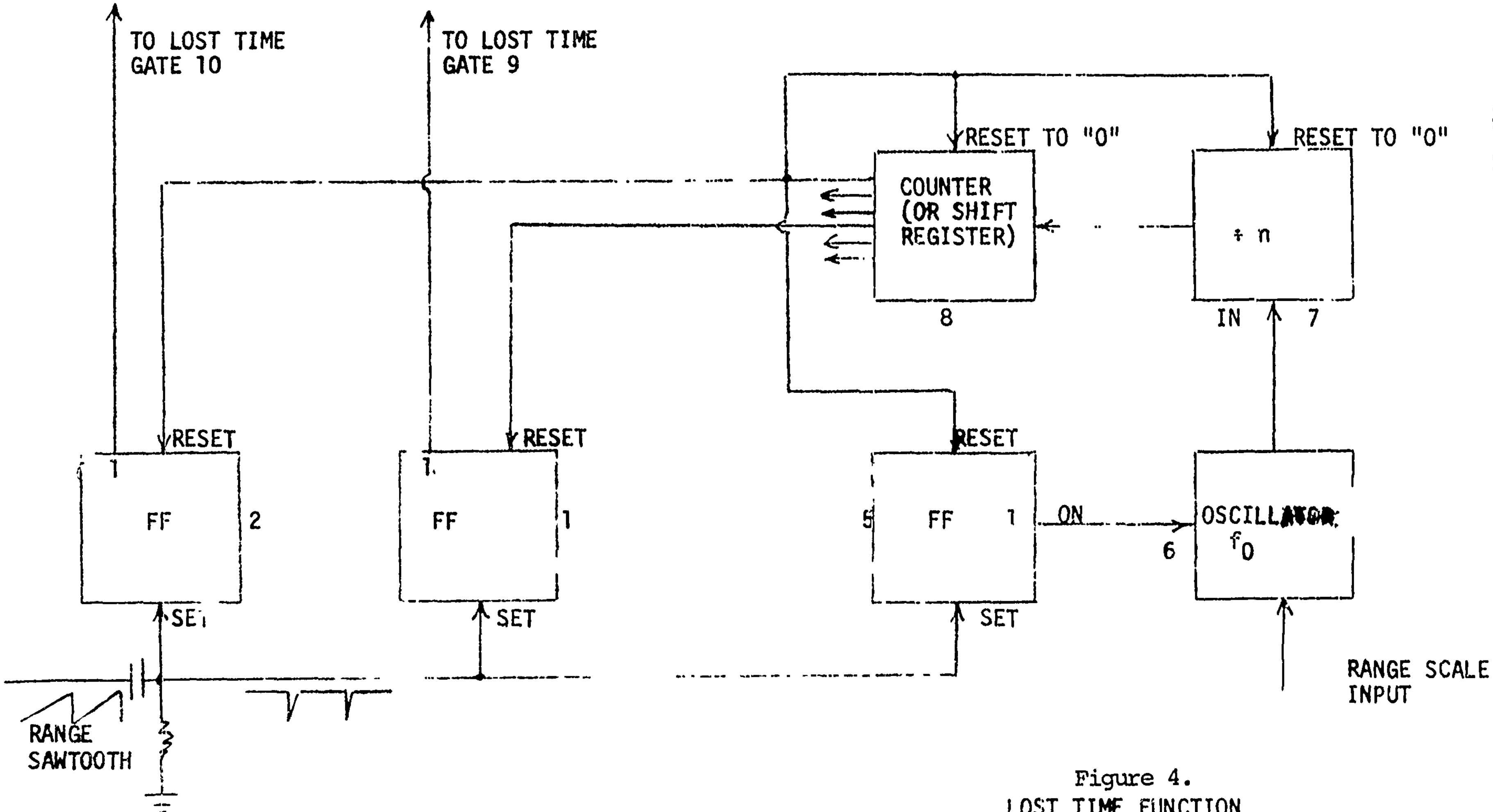

Figure 4.
LOST TIME FUNCTION
GENERATOR

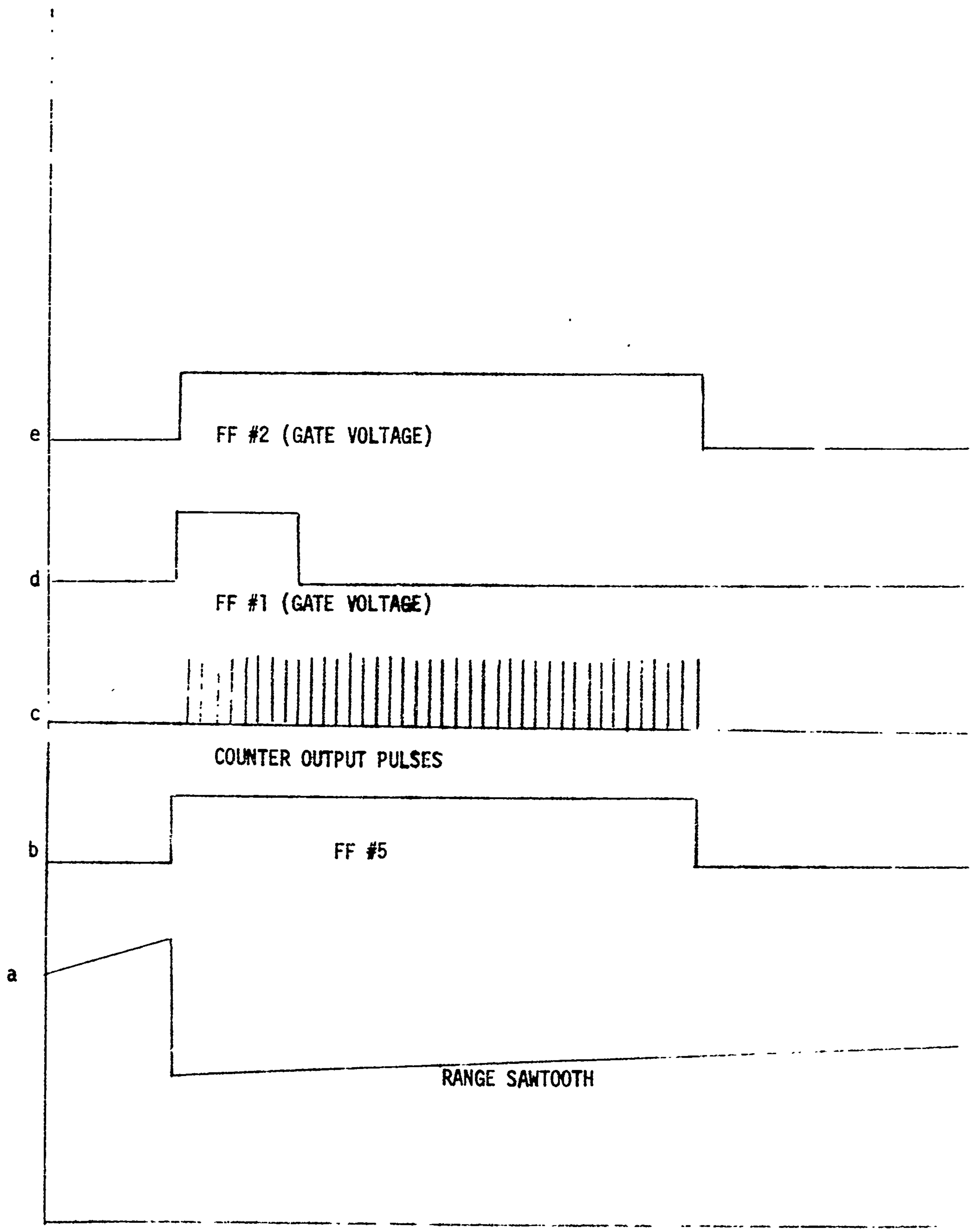

Figure 5.

TIMING DIAGRAM, LOST TIME FUNCTION GENERATOR

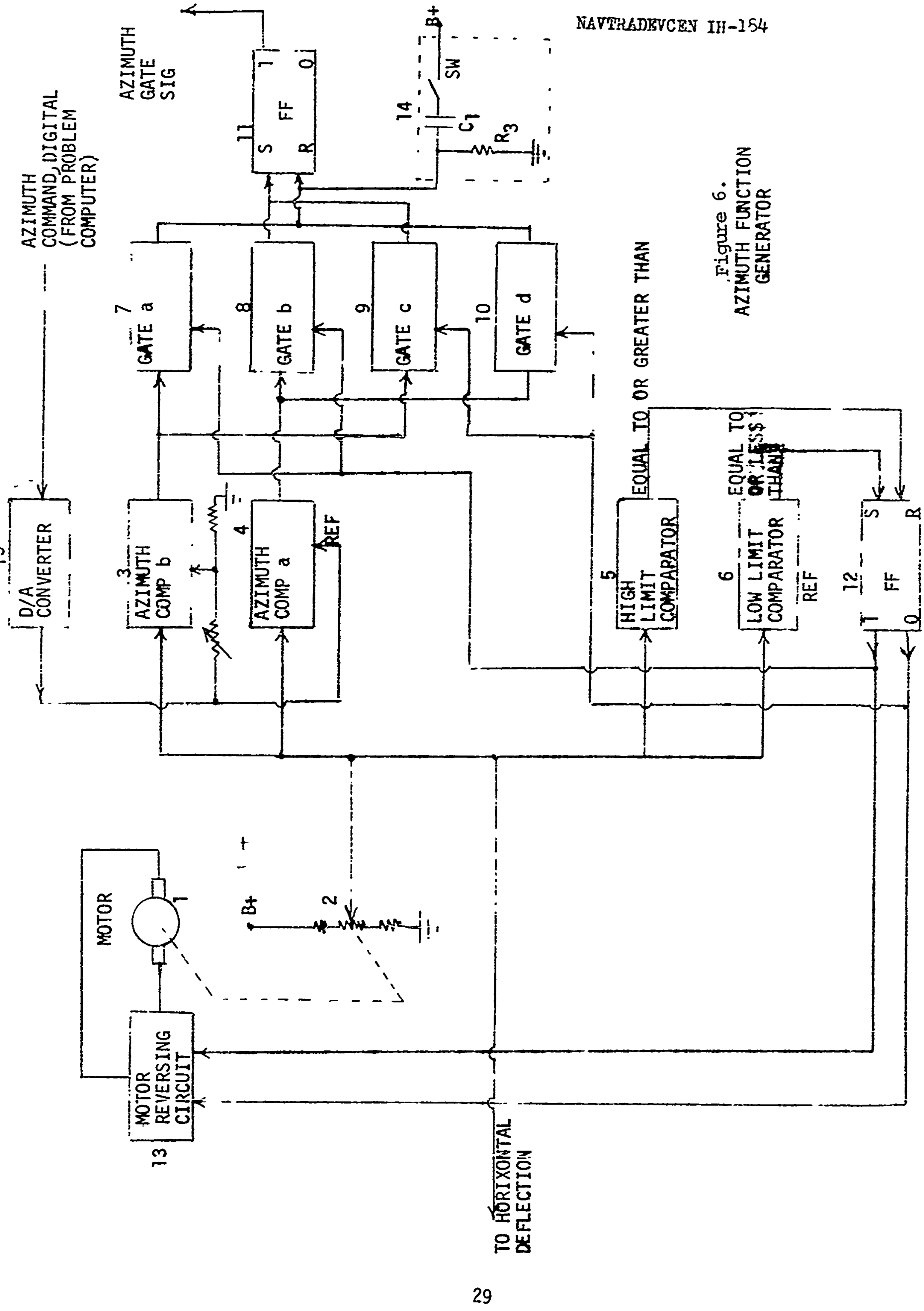

Figure 6.
AZIMUTH FUNCTION GENERATOR

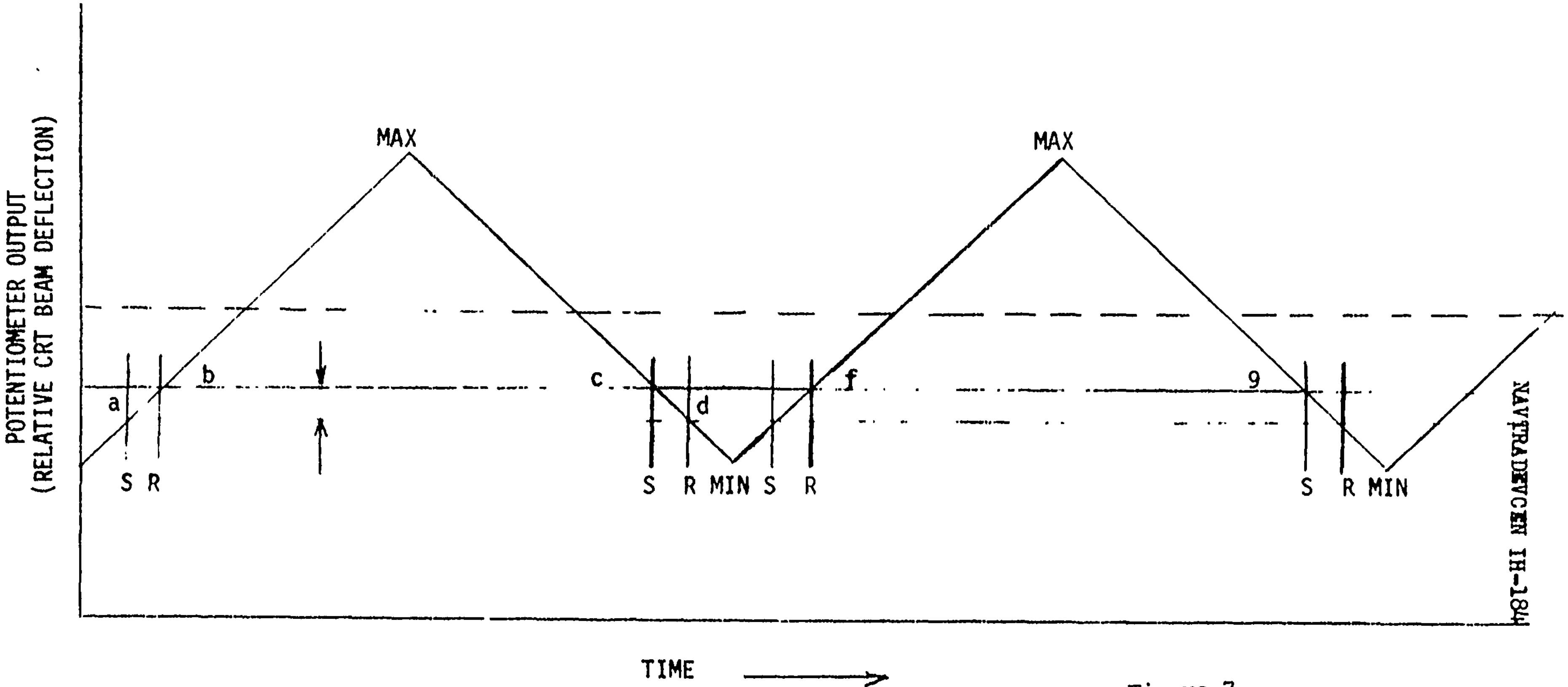

Figure 7.
AZIMUTH DEFLECTION VOLTAGE

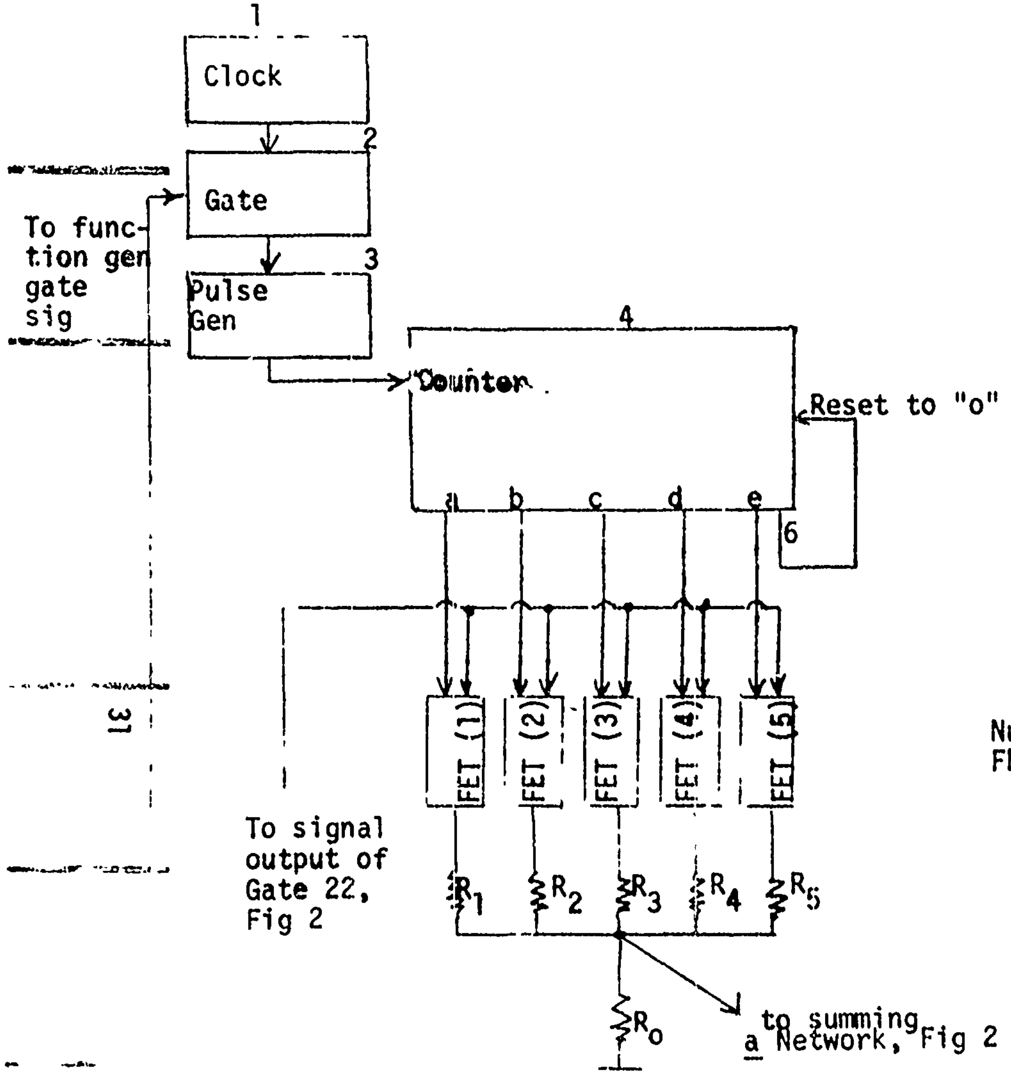

F Figure 8a.
AZIMUTH ATTENUATOR

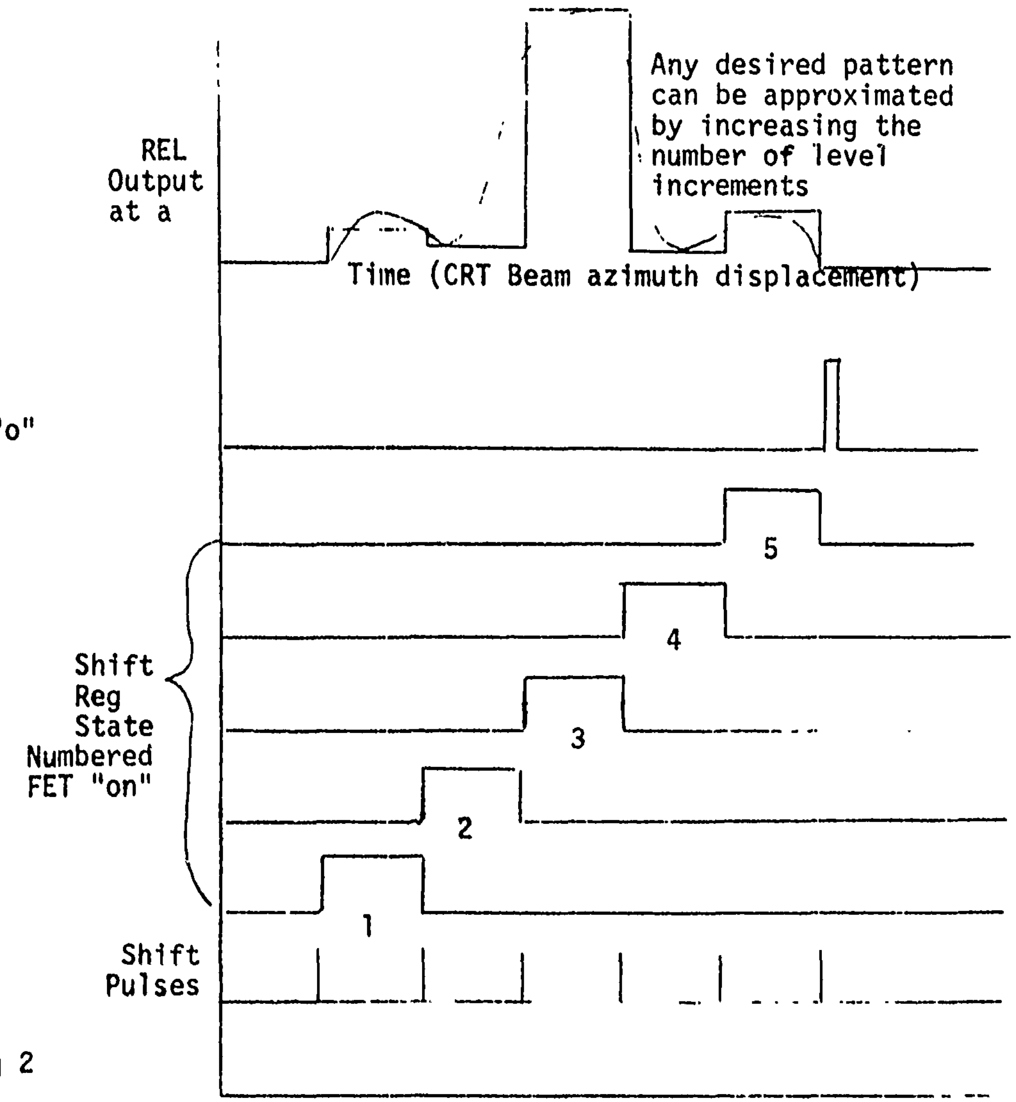

Figure 8b.
TIMING DIAGRAM